DAMTP-2002-144

physics/0211069

An Fe-Si-Ni solidification model of the Earth's layering

A. Aitta*

Department of Applied Mathematics and Theoretical Physics

University of Cambridge

Silver Street, Cambridge CB3 9EW, U.K.

Nov 15, 2002

Abstract

The physical process creating layered structure in planetary rocky bodies is considered here to be multicomponent solidification. This is a unified alternative approach to the present interpretations where each layer is reasoned and matched individually. The Earth's solidification is modelled using the ternary phase diagram Fe-Si-Ni. The four cotectic concentrations and the four corresponding seismic discontinuity radii have been used to show that the silicon concentration as a function of the distance R from the centre of the Earth can be modelled by $C_{Si} = \Gamma(R/R_E)^2$ where $\Gamma = 0.583$, R_E is the Earth's radius and the Ni/Fe ratio is 0.072. Earth would have up to 13 chemically different layers. This model predicts that there are three to four chemically slightly different sublayers in the D" layer and two boundaries in the inner core at radii 870 km and 1050 km. The observed hemispheric asymmetry in the inner core could follow if the Ni-concentration slightly varies locally. Although this model can account for all the layers using only three elements it can not, of course, match the full chemistry of the real Earth.

*e-mail address: A.Aitta@damtp.cam.ac.uk

1 INTRODUCTION

Whether terrestrial objects in their early stages were in a completely molten state or not may be a key determinant for their final state [1]. Here the observed structure of the Earth is considered as have been formed by the solidification process of an initially liquid Earth. Gravity acting with thermal convection is assumed to have quadratically stratified it before the solidification began, rather as the liquid outer core now has a density depending quadratically on the radial distance [10].

The main features of the solidification process occurring in a multicomponent real planet can be modeled using a much simpler fluid system having only a few components. In this paper a ternary system [3, 17] has been used. By having the third component one can reach more realistic conclusions than has been possible previously using a binary solidification model [8]. On the other hand, a more than three component system would be much harder to analyze and compare reliably with the data.

The rocky planets' main two components are silicon and iron. Due to gravity, the lighter Si is predominantly in the mantle and the heavier Fe in the core. Based on meteorite findings it is commonly believed that there is also nickel in the core. This paper considers structure formation in an Earth-size planet made only of three components, namely Fe, Si and Ni. Ni occurs only in a small quantity, but is important in the inner core where it is the most abundant element after Fe. Being lightest, the concentration of Si increases from the centre, while both Fe and Ni have their maximum concentration there. There is no assumption of a complete segregation into a silicon mantle and iron core. However, the assumed quadratic increase of the Si concentration with radius, and similarly decreasing Fe and Ni concentrations, allow the liquid in the outer core to be much enriched in Fe and depleted in Si. Thus Si represents here the light element(s) needed to be present in the outer core to produce the seismically deduced density which is 6-10 % less than that estimated for pure liquid Fe. The identity of the light component(s) has been discussed for 50 years, the discussion being initiated by Birch [5], and all this time Si has been included among the leading candidates [16].

When the planet's surface has cooled enough through thermal radiation into space, surface solidification of Si occurs. The quadratic density profile allows the Si solid crystals to float rather than sink as might occur with a homogeneous density profile. So the solidification front progresses inwards from the surface. The high pressure, despite being combined with high temperature in the centre of the planet, initiates another solidification front starting from the centre and progressing outwards.

These solidification fronts are schematically presented in Fig. 1 where the horizontal axis represents the concentration of the lightest element and the vertical axis represents some solidification parameter λ which depends on both temperature and pressure. Fluid exists only

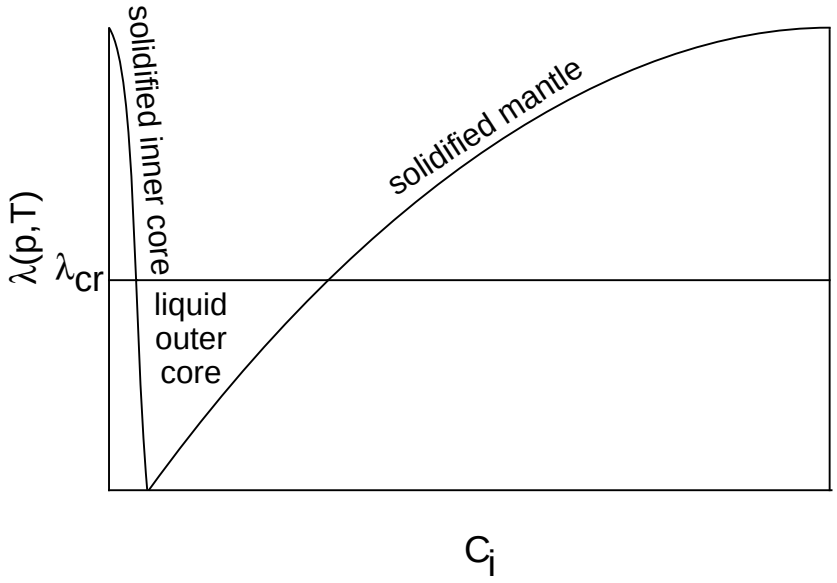

Figure 1: A schematic presentation of a planetary solidification process. The vertical axis indicates some solidification parameter λ which depends on both pressure p and temperature T and C_i is the concentration of the lightest element. A critical value λ_{cr} separates the solidified phases from the liquid phase.

for $\lambda < \lambda_{cr}$, which in the figure is assumed to be the same for both fronts. The details of the solidification product can be seen from the Fe-Si-Ni ternary phase diagram.

2 TERNARY PHASE DIAGRAM OF FE-SI-NI AND THE SOLIDIFICATION PROCESS

Fig. 2 shows the relevant part of the ternary phase diagram of Fe, Si and Ni at normal pressures [17], represented here as having the Fe-corner a right angle. Above its horizontal axis is sketched the Fe-Si binary phase diagram with its temperature dependence shown vertically [17, 4]. It has several critical points on its liquidus surface: between them the crystals precipitating from the liquid would be made of the compound of Fe and Si indicated on the graph, but cocrystallization of the crystals of both neighbouring regimes occurs at the critical points. The Ni component does not influence the concentrations where the Fe-Si binary system has its phase boundaries: they would stay the same whatever the third component was. (See, for instance, the phase diagrams for Fe-Si-O, Fe-Si-Al [4]). All the eutectic type critical points continue as lines inside the ternary phase diagram. Two peritectic critical points P_1 and P_2 are the least well agreed upon [17] and their continuations are omitted although they should be there, too, but they do not have any role for the Earth since their concentrations correspond to the still liquid Earth. Otherwise the liquidus line is reliably established from Fe to Si [17].

The vertical edge, the Fe-Ni binary system, needs to be considered here only for small Ni-concentrations. For k = Ni/(Ni+Fe) ≤ 0.037 there is an Ni-poor δFe(Ni) phase and for $k \geq 0.05$ an Ni-rich γFe(Ni) phase. Between them there is a peritectic regime where both phases occur. These phase boundaries are extended as straight lines into the interior of the phase diagram and they join at (Si, Ni) = (0.04, 0.11) where the peritectic type transition changes to eutectic type [17, 4].

In Fig. 2, the axis of the critical solidification parameter λ should be visualized as perpendicular to the concentration plane similarly as in the simpler Fig. 1. λ depends on both temperature and pressure, combined in such a way that the solidification process, once started, continues: the thermal barriers present in phase diagrams for normal pressures are not obstacles here since they can be overcome by the changing pressure. Thus the thermal barriers do not prevent the liquid line of descent being approximated by a straight line throughout the ternary phase diagram. The liquid planet's initial surface concentration is represented by the point A in Fig. 2. When the liquid is cool enough, Si starts to crystallize out, forming mush: porous solid having residual liquid in its interstices. The released fluid is enriched in Fe and Ni. If there were no convection [2, 3], the residual liquid concentration at the solidification front would follow the linear path moving away from the Si-corner. There the ratio of the Ni to Fe

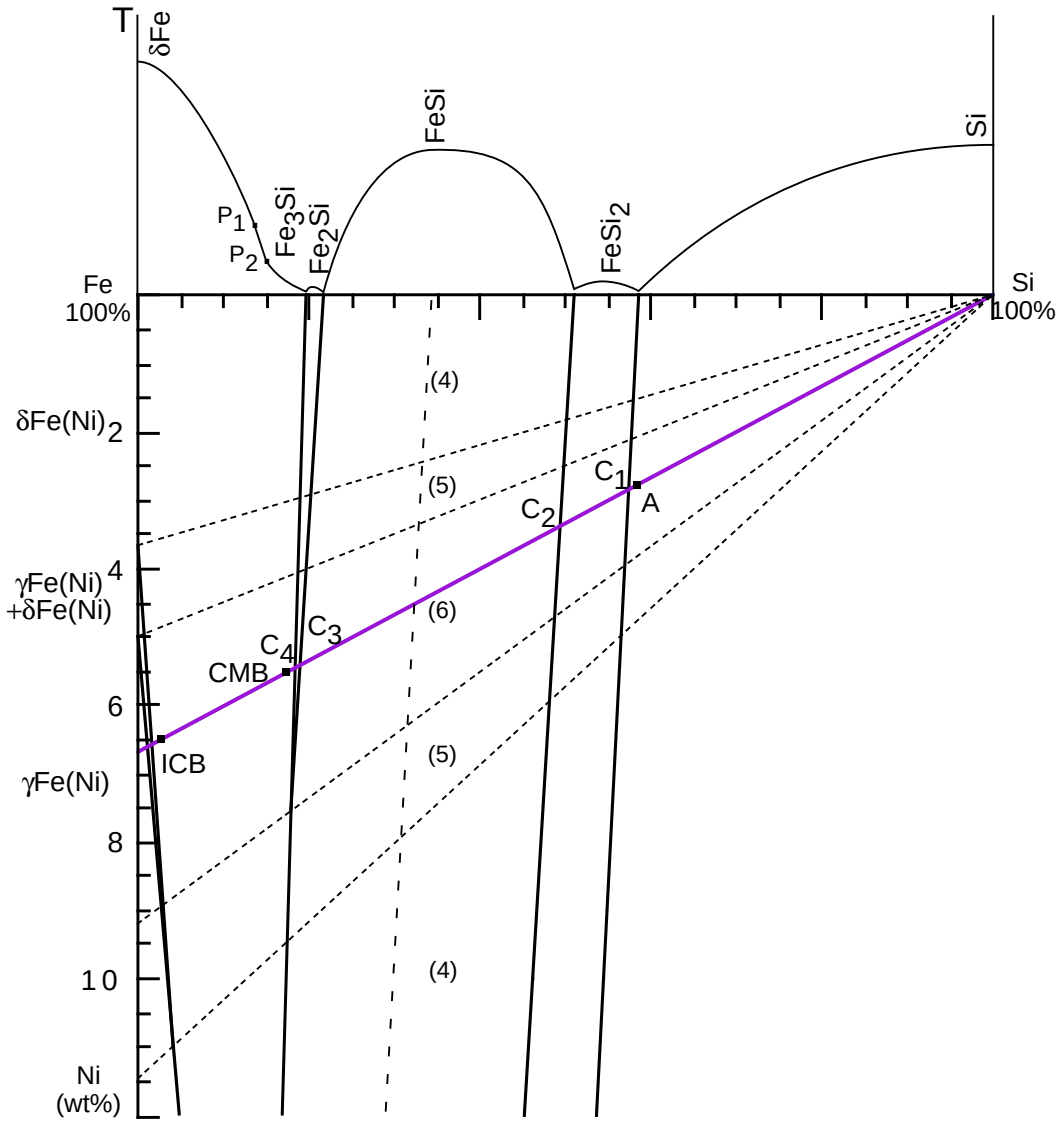

Figure 2: Fe-rich corner of the Fe-Si-Ni ternary phase diagram [17, 4]. Above the horizontal axis the liquidus surface of the Fe-Si binary phase diagram [17, 4] has been sketched with its four eutectic points and its different crystallization products indicated. The eutectic points continue as cotectic lines into the interior of the phase diagram. The Fe-Ni axis has a narrow peritectic region, which has been linearly continued towards the point (Si, Ni)=(0.04, 0.11) where it changes to be a cotectic line. The residual fluid concentration evolves from A (the initial fluid concentration) along the tie line towards C_1 as the Si-mush is solidifying. At C_1 a cotectic mixture of Si and $FeSi_2$ is solidifying. After C_1 the residual fluid evolves along the same tie line towards C_2, C_3, C_4 and on to the CMB, solidifying between them a mushy compound and on each C_j a cotectic mixture of the neighbouring phases. The inner core has been assumed to have started to solidify from the other end of this same line and the residual fluid concentration on its solidification front has now crossed the peritectic region and has reached the ICB (inner core boundary). The liquid line of descent through A corresponds to an Ni/(Ni+Fe) ratio of 0.067. For different planetary bodies the slope of this line (Ni/(Ni+Fe) ratio) could vary and the five possible regions are separated by dotted lines with different selections of the crossed phase boundaries, the number of them being shown in brackets. The dashed line approximates where the solid fraction in the FeSi phase reaches its maximum.

concentration is constant. However, there is both thermal and compositional convection [3] which carry the heavy elements (whose density is similar) down and lighter Si up, holding the concentrations suitably balanced at the front so that the linear path of descent is still followed. When the liquid concentration reaches the first phase boundary at C_1 in Fig. 2, a cotectic crystallization of Si and $FeSi_2$ starts, firstly inside the earlier formed Si-mush, but finally as a new front on its own reaching deeper down than the Si-mush. This cotectic product is also a mush, but its solid fraction is greater than in the Si-mush. The non-solidifying element is Ni, which is the heaviest, and would, if in excess, descend under gravity. Thus the liquid line of descent does not turn along the cotectic line as it would do if there were no convection [2, 3]. Cotectic solidification of Si and $FeSi_2$ continues at C_1 as long as there is enough available Si to crystallize both of them. After that only $FeSi_2$ crystallizes and the residual liquid concentration continues to increase in Fe and Ni along the line C_1C_2. When the concentration reaches the next cotectic line at C_2, cocrystallization of $FeSi_2$ and FeSi occurs as long as there is adequate Si available. When not, the phase FeSi would crystallize alone, releasing only Ni, which descends below the solidification front. The liquid line of descent continues its straight path. The next cotectic line induces at C_3 cocrystallization of FeSi and Fe_2Si, consuming all excess Si. A pure Fe_2Si phase follows as the solidification front moves further down towards the planet's centre. The next crystallization product is the cotectic mixture of Fe_2Si and Fe_3Si at C_4, followed by pure Fe_3Si mush as far as CMB (core-mantle boundary).

For simplicity, the Ni/Fe ratio has been assumed constant along the liquid line of descent, even near the Fe-Ni edge. Any variation induced by the two different solid solutions of Fe(Ni) or by convection is expected to be at most very small. The iron-rich end of the line represents the fluid concentration in the centre of the planet. There the crystallization forms a solid solution of Fe(Ni). When Si is present in small quantities, the solidification of Fe(Ni) increases the amount of Si in the fluid, but since it is the lightest component, it rises. However, a small amount of this residual liquid is trapped in the interstices of the mush. If $k \geq 0.05$ the first solid to form has an Ni-rich γFe(Ni)-structure. When the amounts of Fe and Ni have been consumed sufficiently, there would be simultaneous crystallization of both Ni-rich γFe(Ni) and Ni-poor δFe(Ni). Further solidification of Fe and Ni leads to the phase of Ni-poor δFe(Ni), in the form of mush. If the planet were completely solidified, this outward growing phase would meet the downward growing Fe_3Si phase.

3 QUANTITATIVE RESULTS CORRESPONDING TO THE EARTH

The fluid density in the liquid outer core depends in the PREM model [10] quadratically on radius, and this has motivated the assumption here that the concentration of the initial fluid depends on the radial variable quadratically: Si is increasing from the centre, Fe and Ni are decreasing from their maximum value at the centre to some non-zero value at the surface. The precise quadratic dependence can be inferred from the seismic data as explained below.

All phase boundaries in Fig. 2 are straight lines $C_{Ni} = k_j C_{Si} + b_j$, which are valid for the small values of C_{Ni} considered here, and the values for k_j and b_j for each phase boundary were obtained from the graph in [17] for the four Si-rich lines and from [17, 4] for the two Si-poor lines. The liquid line of descent $C_{Ni} = k(1 - C_{Si})$ crosses these phase boundaries in 4 points if k is less than 0.037, in 5 points if $0.037 \leq k < 0.05$, in 6 points if $0.05 \leq k < 0.092$ and again 5 points for $0.092 \leq k < 0.114$. For bigger k there are only 4 crossing points. These regimes are separated by dotted lines in Fig. 2. The C_{Si} values of these crossing points were sought by changing the slope of the liquid line of descent in steps of 0.001. Their corresponding R-values were estimated as discussed below. The coefficient a in the relationship $C_{Si} = aR^2$, together with k, could then be found by a best fit.

The density discontinuities in the Earth according to the PREM model are presented in Fig. 3. The discontinuities have been identified with the phase changes in the ternary phase diagram. Fig. 3a shows the top 800 km. The outermost layer, crust, varies from 6 km under the oceans to 80 km below the continents, and is shown shaded. In the three-component Earth model the crust has been identified as made of Si crystals. The Si concentration on the cotectic line Si+$FeSi_2$ has been used paired with both $R = 6365$ km (appropriate for oceans) and $R = 6291$ km (appropriate for continents) allowing the fit to find the most suitable thickness for the Si layer. The small density jump seen in PREM at 220 km depth is now known to occur only locally and is not used. The 400 km depth density jump separating the upper mantle from the transition zone has been interpreted as corresponding to the end of the cocrystallization of Si and $FeSi_2$ and to the beginning of the pure $FeSi_2$ phase. This depth is not used in the fit since only the initiation of the cocrystallization concentrations are available in the phase diagram. The next seismic discontinuity, which is much weaker and not visible in PREM, occurs at about 520 km depth, and has been seen in some regions to split into a pair of discontinuities at about 500 km and 560 km [9], also shown shaded in Fig. 3a. This has been identified as the beginning of the cotectic layer of $FeSi_2$+FeSi indicated by the second cotectic line from the right in the phase diagram. All three R-values were used in the fit, with the corresponding Si concentration on this phase boundary, to allow the fit sufficient freedom to address the radial

uncertainty. This cotectic phase would continue until the end of the transition zone. The density jump at 670 km depth has been interpreted as the beginning of the pure FeSi phase which makes up the over 2000 km thick lower mantle, down to the D" layer.

The core-mantle boundary (CMB) region is shown in Fig. 3b. It gives (for $k < 0.092$) two further restrictions for $C_{Si}(R)$. Since in the lowest mantle there is a special, seismically distinct D" layer whose thickness is uncertain but varies from about 100 km up to perhaps 300 km in some places [14], the following interpretation has been made. The CMB was used to estimate where the cotectic crystallization of Fe_2Si and Fe_3Si occurs and the fit was guided by this Si concentration combined with R-values $R_{CMB} = 3483$ km [14] and $R_{CMB} + 100$ km to allow some necessary flexibility in its exact location. The upper edge of the D" layer was sought in the region of the next 100 km (using R-values of 3583 and 3683 km) it being an adequate interval for the data used. It was interpreted to correspond to the beginning of the cotectic crystallization of FeSi+Fe_2Si. These values guided the fit in this region.

The best fit, with the biggest correlation coefficient and the smallest χ^2, was obtained using the Si-concentrations of these four phase boundaries together with the R-values obtained from the seismic and/or density discontinuities, calculated for each slope k (Ni/(Ni+Fe) ratio). The result is that in the fluid $C_{Si} = aR^2$ where $a = (1.437 \pm 0.007).10^{-8}$ km^{-2}, and k= 0.067. This, if scaled by the Earth's radius $R_E = 6371$ km, gives $C_{Si} = \Gamma(R/R_E)^2$ with $\Gamma = 0.583$ which determines the Si-concentration at point A in Fig. 2. The corresponding Ni/Fe ratio is 0.072. The fit, with the points guiding it, is presented in Fig. 4. Also shown is the radial dependence of the other components Ni and Fe, and the radial locations of the phase boundaries and their chemical structure. Using the Si-concentration formula and the Si-concentrations on the two remaining lines in the phase diagram, with the same k, one obtains predictions for two distinct radii (see Fig. 3c and solid dots in Fig. 4) in the inner core where the chemical content and the crystal structure change. The PREM model does not include this possibility. The innermost boundary corresponds to $R = 870$ km and the outer one to $R = 1050$ km. This allows one to interpret the seismically isotropic top 100 - 200 km thick layer of the inner core [11, 12] as the region above $R = 1050$ km made of Ni-poor δFe(Ni) mush whose interstices have fluid in them. The layer between 870 and 1050 km is made of both Ni-rich γFe(Ni) and Ni-poor δFe(Ni) crystals and it belongs to the slightly less isotropic regime in [11]. The innermost core is made of Ni-rich γFe(Ni) crystals and it includes the more anisotropic regime in [11]. On the other hand, there is already seismic analysis giving strong support for a hypothesis of fine-scale structure within the top 300 km of the inner core [21], and describing the increase of anisotropy with depth [19]. The possible hemispheric asymmetry could easily follow if the Ni/Fe ratio is slightly variable locally.

This model gives the (Si, Ni, Fe) fluid concentrations at the inner core surface to be (0.021, 0.066, 0.913), and at the core-mantle boundary (0.174, 0.055, 0.770). The thickness of the D"

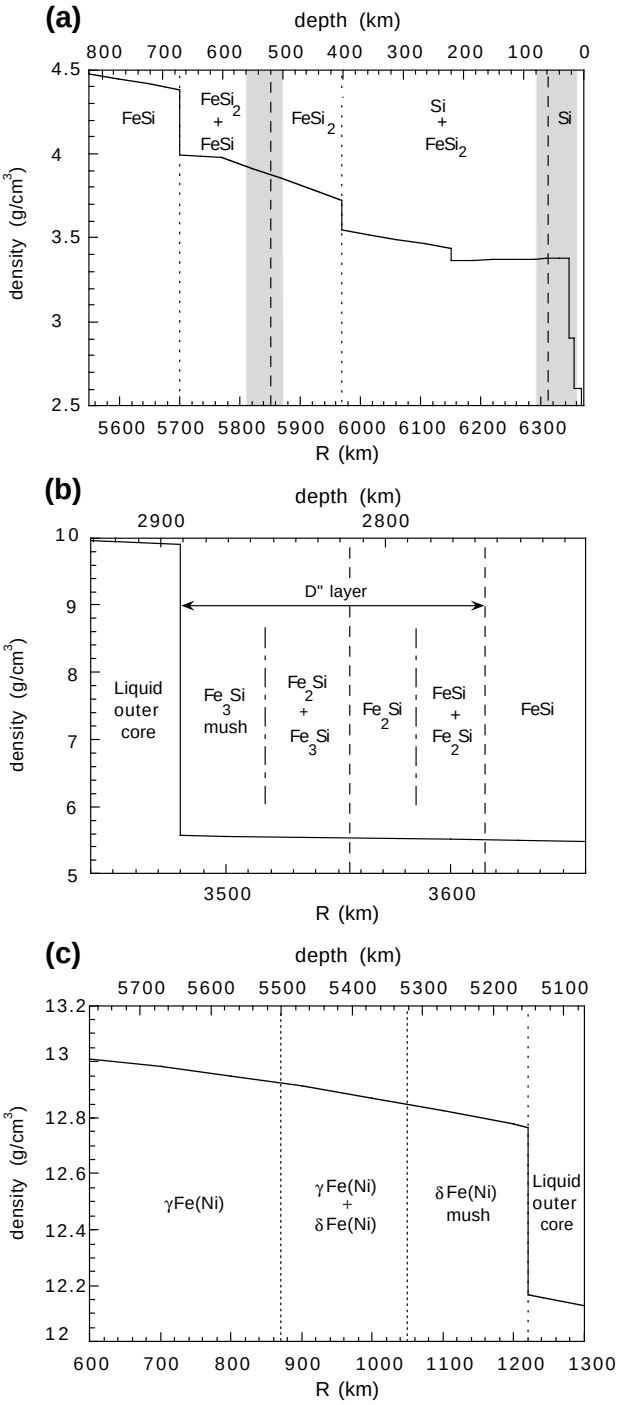

Figure 3: Earth's layered structure and its interpretation using the ternary phase diagram, drawn on the top of the density profile according to the PREM model [10]. (a) The top 800 km of the Earth. Shaded areas indicate the radial regions used by the fit to find a suitable Moho radius and the smaller seismic discontinuity occurring around 520 km depth. The dashed lines are the results from the fit. The bigger density discontinuities, marked as dotted lines, have been interpreted to be the end radii of the cotectic crystallization. (b) Region at the bottom of the mantle. PREM indicates only the CMB density jump. The D" layer was identified to consist of at least the Fe_2Si phase with its cotectic neighbouring phases. Its lower radius was sought within 100 km of the CMB and its upper radius in the next 100 km above. The dashed lines are the results from the fit. The lower radii of the cotectic layers can not be determined by the model, the dashed-dotted lines are just indications that those boundaries should be somewhere there. (c) The inner core structure predicted by this model.

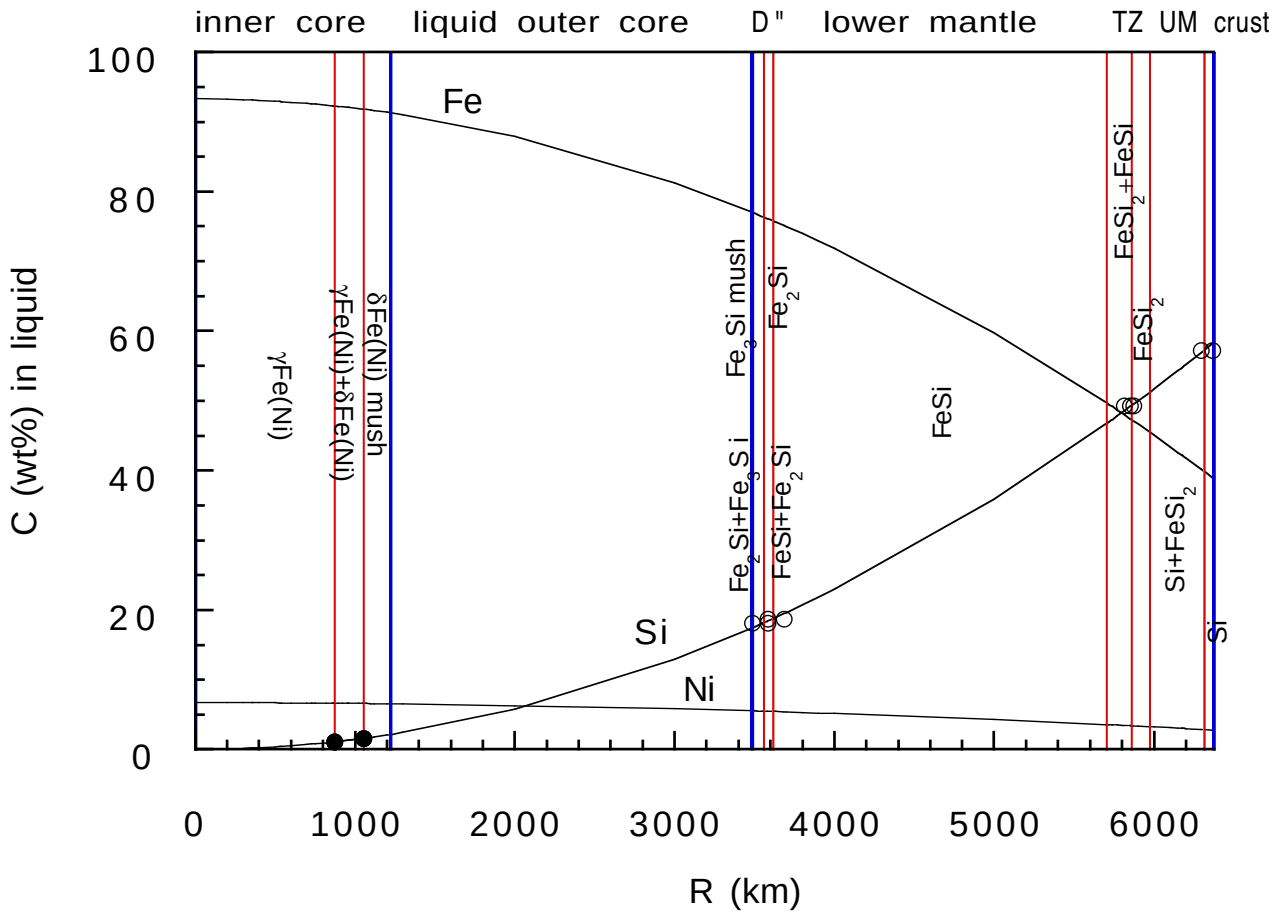

Figure 4: Fluid concentrations C as a function of the radius at the solidification front. The fit is $C_{Si} = aR^2$ with the points used in the fit marked as open circles. This best fit was obtained with Ni/(Ni+Fe) = 0.067, this allows the calculation of the other elements' concentrations C_{Fe} and C_{Ni}. The vertical lines separate the layers found in this model and their chemical structure. The two solid dots indicate the Si-concentrations and radii of the structure change predicted by this model inside the inner core. The fronts at the present time are marked with bolder lines.

layer is determined by the fit to be 132 km which agrees very well with seismic measurements [21]. Its uppermost region is made of a cotectic mixture of FeSi and Fe_2Si and below it is a layer of Fe_2Si, but the location of their boundary is not available from the model. The core-mantle boundary is located 72 km below the start of the next layer, cotectically crystallizing Fe_2Si and Fe_3Si whose thickness is not known, but is unlikely to be very wide, so that at the present time the front is probably crystallizing Fe_3Si mush as schematically shown in Fig. 3b.

4 DISCUSSION AND CONCLUSIONS

The silicate-rich outer parts and iron-rich inner parts of the planets are the product of multicomponent solidification. Only partial differentiation of the heavy and light elements needs to have occurred. It would have been enough that gravity with convection initially stratified the fluid in a continuous manner. Here this stratification has been shown to depend on the second power of the radial distance.

The Earth, if modeled by only the three components Fe, Si and Ni, with the Ni/(Ni+Fe) ratio at the solidification front having a constant value 0.067, would generate 13 chemically different layers just via the process of three-component solidification. The layers are shown in Table 1, but omitted from the Table is that each layer after the outermost and innermost would first grow in the interstices of the previous mush. This could reduce the sharpness of the boundaries. Since the layers in multicomponent solidification are knit together by mush growth the thermal boundary layers, expected to occur for sharp chemical layering, would be absent. In addition, close to the middle of the one-component phases the solid fraction of the primary phase reaches its maximum, and this might have been observed in some measurements about 1000 km above the CMB [20]. Here it is estimated to occur at about $R = 4720$ km, 1237 km above the CMB.

The phase diagram lets one estimate the fluid concentrations where each cotectic layer first appears without the previous mush (for a constant Ni/Fe ratio). Their radial locations have been obtained by making an identification to seismic discontinuities. The model gives estimates for the fluid concentrations anywhere in the liquid outer core and especially at the inner core and core-mantle boundaries. In the outer core the Si-concentration is on average about 11 wt% which agrees very well with the density expectations based on seismic measurements [6].

Similar abundances occur in the Sun. The Si/Fe ratio in the Sun is 0.561 as calculated using data in [7]. In this Earth model Si/Fe is 0.577 if averaged without any density profile correction, or 0.520 if a very simple radial density profile correction is employed, both rather close of the solar value.

This model gives a new, very satisfactory account of the physical and chemical basis of

the well-documented seismic layered structure of the Earth. The multitude of elements and chemicals in the real Earth could possibly increase the number of layers, but it is not likely that any of the layers described in this paper disappear, since they follow directly from the binary system of Fe-Si except in the inner core where they follow from the binary system Fe-Ni. The chemical content of the real Earth is, of course, enriched by the presence of the other elements. This model considers only the initial solidification at the liquidus surface and does not take into account any later events like late impacts or the recycling of the Earth's crust into the mantle at subduction zones, which affect the chemical structure of the topmost layers.

The seismic discontinuities at 400 and 670 km depth are identified here with chemical changes, not pressure-induced structural changes. The transition zone has here two chemically different layers: the upper one corresponds to $FeSi_2$ while the lower one has a mixture of $FeSi_2$+FeSi. The real chemical structure in these upper layers is known to be much modified by the presence of many more elements and the substantial recycling and recrystallisation of the materials. The model, however, agrees with the chemical type of the lower mantle: generally assumed to be dominantly $(Mg,Fe)SiO_3$ with perovskite structure. This corresponds to FeSi in this simplified model with only three components. Further inclusion of the two next commonest elements, namely O and Mg, would agree fully with our previous conceptions of the chemical compounds dominating the lower mantle. Additional lighter elements are, of course, needed to account for the mantle density in the real Earth, and their solidification is expected to have occurred in the interstices of the first solidified dominating compounds, thus generating also anisotropy.

This model sheds light on the physical mechanism behind some seismic observations in the middle of the lower mantle. The solid fraction of FeSi-mush reaches its maximum at depth of about 1650 km (dashed line in Fig. 2). It would act as a barrier of some strength to material flow although there is no change in chemical composition across it, only in the relative abundance of FeSi. A seismic low-velocity layer [13] has been observed to occur at depths 1400 - 1600 km. Structural and chemical heterogeneity [20] has been suggested to occur below this barrier at depths 1700 - 2300 km. This heterogeneity is probably a consequence of the appearance of the cotectically crystallized FeSi and Fe_2Si in the interstices of the FeSi mush.

The D" layer has previously been anticipated to be chemically different from the lower mantle by some authors [18] even if its structure has not yet been agreed upon. The observed 40-60 km thick ridge-like ultra low velocity zone [15] is probably due to the uneven [2] gupeiite (Fe_3Si) mushy layer surface.

The crystal structure of Fe at high pressures is supposed to change from δ to ϵ. There are not adequate measurements to indicate if this happens also for Fe(Ni) at the inner core

Depth (km)	Radius (km)	Layer	Chemical compounds
(0)-59	(6371)-6312	crust	Si
59-(400)	6312-(5971)	upper mantle	Si+$FeSi_2$
(400)-513	(5971)-5858	upper transition zone	$FeSi_2$
513-(670)	5858-(5701)	lower transition zone	$FeSi_2$+FeSi
(670)-2756	(5701)-3615	lower mantle	FeSi
2756–	3615–	upper D" layer	FeSi+Fe_2Si
–2816	–3555	middle D" layer	Fe_2Si
2816–	3555–	lower D" layer	Fe_2Si+Fe_3Si
–(2888)	–(3483)	lowest D" layer	Fe_3Si-mush
(2888)-(5150)	(3483)-(1221)	outer core	Fe+Ni+Si solution
Inner core:			
(0)-171	(1221)-1050	outermost inner core	Ni-poor δFe(Ni) mush
171-351	1050-870	middle inner core	δFe(Ni) + γFe(Ni)
351-(1221)	870-(0)	innermost inner core	Ni-rich γFe(Ni)

Table 1: Earth's layering. Numbers without brackets come from this model.

pressures and at the liquidus temperature. But even if both structures γ and δ change to be ϵ at high pressures, the phases would be different due to their different Ni-concentrations: the deepest inner core is rich in Ni, the outermost mushy layer is poor in Ni and the layer between is a heterogeneous mixture of Ni-rich and Ni-poor Fe.

ACKNOWLEDGMENTS

I thank Michael Carpenter, John Hudson and Dan McKenzie for discussions. The main results of this work were presented as part of a poster "Ternary solidification and beyond" at the 10th Anniversary Symposium of the Daphne Jackson Trust on 21.1.2002 at the University of Surrey, Guildford, Surrey.

References

[1] Agee, C. B., 1993. Introduction to the special section on magma oceans. *J. Geophys. Res.*, **98**, 5317.

[2] Aitta, A., Huppert, H. E. and Worster, M. G., 2001a. Diffusion–controlled solidification of a ternary melt from a cooled boundary. *J. Fluid Mech.* **432**, 201–217.

[3] Aitta, A., Huppert, H. E. and Worster, M. G., 2001b. Solidification in ternary systems. in *Interactive dynamics of convection and solidification* pp. 113–122, eds. Ehrhard, P., Riley, D. S. and Steen, P. H., Kluwer, Dordrecht.

[4] ASM Handbook Vol. 3 *Alloy Phase Diagrams*, 1992. ed. Baker, H., ASM International, Metals Park, Ohio.

[5] Birch, F., 1952. Elasticity and constitution of the Earth's interior. *J. Geophys. Res.*, **57**, 227–286.

[6] Birch, F., 1964. Density and Composition of Mantle and Core. *J. Geophys. Res.*, **69**, 4377–4388.

[7] Bahcall, J. N. and Pinsonneault, M. H., 1995. Solar models with helium and heavy-element diffusion. *Rev. Mod. Phys.* **67**, 781–808.

[8] Braginsky, S. I., 1963. Structure of the F layer and reasons for convection in the Earth's core. *Dokl. Akad. Nauk. SSSR* (Earth Science) **149**, 8–10.

[9] Deuss, A. and Woodhouse J., 2001. Seismic observations of splitting of the mid-transition zone discontinuity in Earth's mantle. *Science* **294**, 354–357.

[10] Dziewonski, A. M. and Anderson, D. L., 1981. Preliminary reference Earth model. *Phys. Earth Planet. Inter.* **25**, 297–356.

[11] Garcia, R. and Souriau, A., 2000. Inner core anisotropy and heterogeneity level. *Geophys. Res. Lett.* **27**, 3121–3124.

[12] Garcia, R. and Souriau, A., 2001. Correction to "Inner core anisotropy and heterogeneity level" by R. Garcia and A. Souriau. *Geophys. Res. Lett.* **28**, 85–86.

[13] Kaneshima, S. and Helffrich, G., 1999. Dipping low-velocity layer in the mid-lower mantle: evidence for geochemical heterogeneity. *Science* **283**, 1888–1891.

[14] Masters, T. G. and Shearer, P. M., 1995. Seismic models of the Earth: Elastic and Anelastic. *Global Earth Physics: Handbook of Physical Constants* p. 94, ed. Ahrens, T. J. AGU, Washington.

[15] Ni, S. and Helmberger, D. V., 2001. Probing an ultra-low velocity zone at the core mantle boundary with P and S waves. *Geophys. Res. Lett.* **28**, 2345–2348.

[16] Poirier, J.-P. *Introduction to the Physics of the Earth's interior, 2nd Ed.* (Cambridge University Press, Cambridge 2000).

[17] Raynor, G. V. and Rivlin, V. G., 1985. Critical evaluation of constitution of cobalt-iron-silicon and iron-nickel-silicon alloys. *Intern. Metals Rev.* **30**, 181–208.

[18] Sidorin, I. and Gurnis, M., 1998. Geodynamically consistent seismic velocity predictions at the base of the mantle. *Geodynamics* **28**, 209–230.

[19] Song, X. and Helmberger, D. V., 1998. Seismic evidence for an inner core transition zone. *Science* **282**, 924–927.

[20] van der Hilst, R. and Karason, H., 1999. Compositional heterogeneity in the bottom 1000 kilometers of Earth's mantle: towards a hybrid convection model. *Science* **283**, 1885–1888.

[21] Vidale, J. E. and Benz, H. M., 1993. Seismological mapping of fine structure near the base of the Earth's mantle. *Nature* **361**, 529–532.

[22] Vidale, J. E. and Earle, P. S., 2000. Fine-scale heterogeneity in the Earth's inner core. *Nature* **404**, 273–275.